

# Transportation efficiency of hydrodynamically coupled spherical oscillators in low Reynolds number fluids

Weiwei Su\*

*Department of Mathematical Informatics, The University of Tokyo, Bunkyo City, Tokyo 113-8654, Japan*

Yuki Izumida<sup>†</sup> and Hiroshi Kori<sup>‡</sup>

*Department of Mathematical Informatics, The University of Tokyo, Bunkyo City, Tokyo 113-8654, Japan and*

*Department of Complexity Science and Engineering,  
The University of Tokyo, Kashiwa, Chiba 277-0882, Japan*

(Dated: April 21, 2023)

Most bacteria are driven by the cilia or flagella, consisting of a long filament and a rotary molecular motor through a short flexible hook. The beating pattern of these filaments shows synchronization properties from hydrodynamic interactions, especially in low Reynolds number fluids. Here, we introduce a model based on simple spherical oscillators which execute oscillatory movements in one dimension by an active force, as a simplified imitation of the movements of cilia or flagella. It is demonstrated that the flow, measured by the net transportation of a test particle, is generated by a chain of oscillators and enhanced by the hydrodynamic interactions between beads, with supports from both perturbative and numerical results. Transportation efficiency also highly correlates with hydrodynamic interactions. Increments of bead numbers are generally expected to produce stronger flow and efficiency, at least for small numbers of beads.

## I. INTRODUCTION

The cilia and flagella are the fundamental organs for microorganisms as the instruments of swimming in low Reynolds number environments [1, 2] and transporting materials like protein [3]. The undergoing mechanics in their wave-like behaviors is also a perfect paradigm for the study of active matter [4]. The synchronization of the beating pattern of these filaments is common [5]. Usually, for example, bacteria perform a two-gait “run-and-tumble” motion in fluids [6]. From repeating such motion the bacteria gain the net momentum in order to move. Thus it is worth investigating the mechanism behind such behavior in an analytical interpretation.

Some experimental studies take efforts to discover the relation between viscous hydrodynamic interaction and synchronization, as Taylor originally proposed [7]. Experiments on carpets of bacteria with active flagella [8] and arrays of artificial magnetically actuated cilia [9–11] have found collective effects via hydrodynamic interactions such as complex flow patterns and collective phase shifts. Through the synchronization of filaments, it is well known that the energy dissipation of the model can be minimized [12], so one can expect that such collective effects provide sufficient influence over the performance of the oscillator model.

The dynamic of passively induced movement generated by the flagella is a highly complex elasto-hydrodynamic problem [13]. Therefore, in order to solve such a model, a computationally simple but still practically accurate model is required. It has been a popular idea of representing slender filaments by spheres for hydrodynamic modeling [14]. Uchida and Golestanian propose a generic criterion to reach stabilized states for two beads with arbitrary but periodic trajectory and force profile [15]. Recently, the details of hydrodynamic effects are categorized by direct and indirect effects from the slender structure of filaments, from approximating the filament as a point mass orbiting around the cell [16].

One representative of a minimal model can be found in Ref. [17]. In this literature, a pair of spherical beads orbiting in the same shape of periodic trajectory near a wall is investigated. At first, the linear stability of the synchronized state is analyzed and examined by, for instance, circular, linear, and elliptical trajectories. Furthermore, the analysis of nonlinear evolution for these trajectories is done in the far-field limit, as well as their near-field interaction between two beads due to the finite size of the trajectory.

For a better comprehension of the low Reynolds number hydrodynamics, there are literatures such as Kotar et al. [18], which focuses on the optimal condition of hydrodynamic synchronization for rotors in circular trajectories. This article numerically examines the model setups proposed by Niedermayer et al. [19] and Uchida & Golestanian [15],

---

\* The author is now belonging to Department of Complexity Science and Engineering, The University of Tokyo, Kashiwa, Chiba 277-0882, Japan; Email: su-weiwei@g.ecc.u-tokyo.ac.jp

<sup>†</sup> Email: izumida@k.u-tokyo.ac.jp

<sup>‡</sup> Email: kori@k.u-tokyo.ac.jp

that a smaller spring stiffness or larger asymmetry leads to stronger coupling condition and synchronization. Another conclusion is, if some thermal noise is included in the original setup, the synchronization still holds for not very high temperatures. Liao & Lauga [20] have examined a model of two spherical bodies in circular orbits of late as well, and the condition of minimal energy dissipation rate is discovered.

In this article, we build a simple model, namely, a chain of spherical beads that oscillate in a one-dimensional orbit and are hydrodynamically coupled with one another, and focus on the transportation efficiency of the system, which is rarely focused on by previous literature. Our results are expected to contribute to describe the ciliary motion in mucociliary transport of the respiratory system and oviduct transport of the female reproductive system [21–24]. Moreover, the metachronal pattern we discovered in the case of many beads provides theoretical implications for some motion generated from motile cilia in bacteria like *Paramecium* cells [25].

The flow of text is as the following: We will first introduce a minimal model, with only two beads inside. In the two-bead model, we provide the theoretical analysis of the dynamical system using a perturbation method, yielding expressions for net transportation, work, and efficiency. We then numerically analyze the case of many beads, indicating the positive cooperative effect via hydrodynamic interaction between the beads.

## II. THE GENERAL SETUP

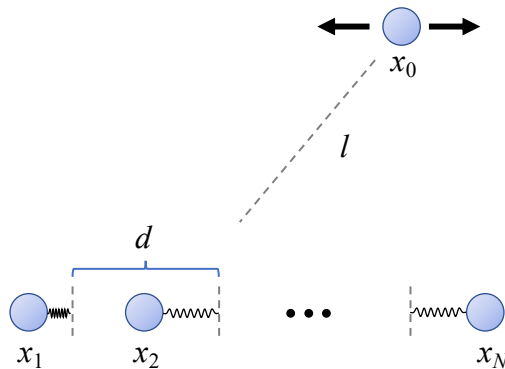


FIG. 1. The setup of spherical bead model. Here,  $d$  is the distance between the equilibrium positions of neighboring beads;  $l$  is the typical distance between the beads and the test particle.

As an analytically tractable model of a flow generator, a one-dimensional setup is established and illustrated in Fig. 1. Specifically, consider  $N$  spherical beads that can move only along the  $x$ -axis, obeying

$$\gamma [\dot{x}_i - v(x_i)] = F_i, \quad (1)$$

where  $\gamma = 6\pi\mu a$  is the drag coefficient for the fluid viscosity  $\mu$ ,  $a$  is the radius of the beads,  $x_i$  ( $i = 1, 2, \dots, N$ ) is the position of bead  $i$ ,  $v(x_i)$  is the flow field at  $x_i$  generated by the beads  $j \neq i$ , and  $F_i$  is the active force applied to bead  $i$ . The flow field is given by

$$v(x_i) := \sum_{j \neq i} H_{ij} F_j, \quad (2)$$

where  $H_{ij}$  ( $1 \leq i, j \leq N$ ) is the Oseen tensor for the Stokeslet in incompressible Newtonian fluid [26]. Because only one-dimensional motion in the  $x$ -direction is considered, the Oseen tensor is given as

$$H_{ij} = \frac{1}{\gamma} \frac{3a}{2|x_{ij}|} + O\left[\left(\frac{a}{d}\right)^3\right], \quad (3)$$

where  $x_{ij} = x_i - x_j$  and  $d$  is the distance between the equilibrium positions of the neighboring beads. Hereafter, all  $O\left[\left(\frac{a}{d}\right)^3\right]$  terms are neglected. Also consider a test particle of radius  $a$ , obeying

$$\gamma [\dot{x}_0 - v(x_0)] = 0, \quad (4)$$

where

$$v(x_0) := \sum_{j=1}^N H_{0j} F_j, \quad (5)$$

$v(x_0)$  is the velocity profile of the test particle. Denote the typical distance between the flow generator and the test particle by  $l$ . Here, we assume  $l \gg d$  and employ the following approximation throughout this study:

$$H_{0j} = \frac{1}{\gamma} \frac{3a}{2l}. \quad (6)$$

With this approximation,  $l$  only affects the magnitude of displacement of  $x_0$  and can be chosen arbitrarily. Active force  $F_i$  is modeled as follows. Assume that each bead is connected to a pinned point by an elastic beam, which exerts force by periodically changing its natural length. Specifically, consider

$$F_i = k [x_i^* + L(\phi_i) - x_i], \quad (7)$$

$$L(\phi_i) = \epsilon L_0 \sin \phi_i, \quad (8)$$

$$\phi_i = \omega t + \psi_i \quad (9)$$

where  $x_i^* + L(\phi_i)$  is the equilibrium position,  $L(\phi_i)$  is the change of the natural length,  $\phi_i$  is the phase of beating,  $k$  is the spring constant,  $\psi_i$  is the phase offset, and  $\epsilon L_0$  is the oscillation amplitude of the natural length,  $\epsilon$  is a nondimensional quantity introduced for later convenience. Without loss of generality, set  $x_i^* = (i-1)d$  and  $\psi_1 = 0$ . One can interpret that beams repeat contraction and expansion with period  $T = \frac{2\pi}{\omega}$  with some phase differences between the neighbors. In the following numerical simulations, without specific mentions we fix numerical values of parameters as:  $a = 0.1$ ,  $\gamma = 1$ ,  $l = 1000$ ,  $L_0 = 1$ ,  $\omega = 1$  and vary  $N$ ,  $d$ ,  $\epsilon$  and  $\psi_i$  ( $i = 2, \dots, N$ ). Typical behavior for  $N = 4$  is displayed in Fig. 2.

To quantify the system performance, define the following efficiency for the transportation of the test particle:

$$\hat{\eta} := \frac{\gamma \langle v_0 \rangle^2}{P} = \frac{\gamma R^2}{WT}, \quad (10)$$

where  $\langle \cdot \rangle$  denotes the average over one cycle,  $P$  and  $W$  are the total power and work exerted by the flow generator for one cycle, respectively, and  $R$  is the net transportation of the test particle for one period. More precisely, define

$$R := \lim_{n \rightarrow \infty} \int_{nT}^{(n+1)T} \dot{x}_0 dt = \lim_{n \rightarrow \infty} \int_{nT}^{(n+1)T} v(x_0) dt = \lim_{n \rightarrow \infty} \frac{3a}{2\gamma l} \int_{nT}^{(n+1)T} \sum_{j=1}^N F_j dt, \quad (11)$$

where  $n$  is the number of cycles and consider a large  $n$  limit to eliminate the transient behavior. Also define

$$W := \sum_{i=1}^N W_i, \quad (12)$$

where

$$W_i := \lim_{n \rightarrow \infty} \int_{nT}^{(n+1)T} (\dot{x}_i - v(x_i)) F_i dt = \lim_{n \rightarrow \infty} \frac{1}{\gamma} \int_{nT}^{(n+1)T} F_i^2 dt. \quad (13)$$

One may evaluate  $R$ ,  $W$ , and thus  $\hat{\eta}$  if the time-asymptotic behavior of  $x_i(t)$  ( $i = 1, \dots, N$ ) is obtained.

We are interested in the cooperative effect on the efficiency and thus later compare the efficiency for different  $N$  values. Thus, it is convenient to introduce the per-unit efficiency:

$$\eta = \frac{\hat{\eta}}{N} = \frac{\gamma R^2}{WTN}. \quad (14)$$

A positive cooperative effect is indicated if  $\eta$  significantly increases with  $N$ .

A similar kind of efficiency could be found, such as the Lighthill hydrodynamic efficiency (cf. Ref. [27]) which happens to be one of the most popular among literatures (for instances, in Ref. [28, 29]). There, the particle is approximately spherical and deformable in order to move by morphing and the expression is

$$\hat{\eta}' := \frac{\gamma \langle v_0 \rangle^2}{\langle P \rangle} \quad (15)$$

where  $v_0$  is the velocity of the particle and  $P$  is the work done from morphing. This is fundamentally the same definition as ours if one replaces the work done from morphing to the work done by beads.

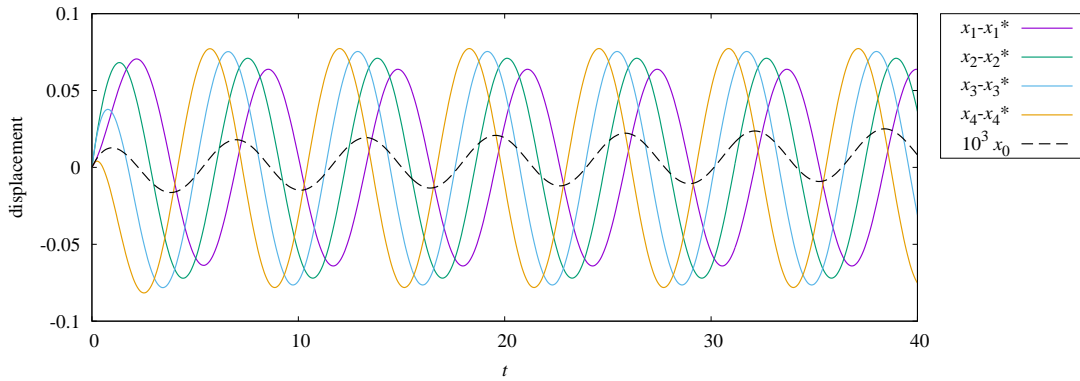


FIG. 2. Typical dynamical behavior of the system for  $N = 4$ ,  $\psi_i = 1.0(i-1)$ ,  $d = 1$  and  $\epsilon = 0.1$ . The displacements of the beads,  $x_i - x_i^*$  ( $i = 1, 2, 3, 4$ ), are plotted together with that of the test particle,  $10^3 x_0$  (instead of  $x_0$  for visibility). The amplitudes of beads are different because of the effect of hydrodynamic coupling. The slope of the envelope of  $x_0$  is approximately  $R/T$ .

### III. THE MINIMAL MODEL: A 2-BEAD CASE

Here, by considering the minimal model, the flow generator consisting of only two beads ( $N = 2$ ), and perturbatively solving such system, we derive the expressions for  $R, W$ , and  $\hat{\eta}$ . For simplicity,  $\psi_2$  is denoted as  $\psi$  in this section; thus,  $\phi_1 = \omega t$  and  $\phi_2 = \omega t + \psi$ . Then, our model for  $N = 2$  is

$$\dot{x}_1 = \frac{3a}{2\gamma|x_2 - x_1|} F_2 + \frac{1}{\gamma} F_1, \quad (16a)$$

$$\dot{x}_2 = \frac{3a}{2\gamma|x_2 - x_1|} F_1 + \frac{1}{\gamma} F_2. \quad (16b)$$

The perturbation method might be applied by treating  $\epsilon$  as a small parameter. Firstly introduce the dimensionless version of canonical basis as

$$X := \frac{x_1 + x_2}{d}, \quad (17)$$

$$Y := \frac{x_2 - x_1}{d}. \quad (18)$$

For simplicity, always assume  $Y > 0$ , which is a reasonable assumption physically, meaning that the beads never overlap with each other, so no collision occurs. Then, Eq. (16) becomes

$$\dot{X} = \frac{k}{\gamma} \left( \frac{3a}{2dY} + 1 \right) \left[ 1 + \epsilon \hat{L}_0 (\sin \phi_1 + \sin \phi_2) - X \right], \quad (19a)$$

$$\dot{Y} = \frac{k}{\gamma} \left( -\frac{3a}{2dY} + 1 \right) \left[ 1 + \epsilon \hat{L}_0 (\sin \phi_2 - \sin \phi_1) - Y \right], \quad (19b)$$

where  $\hat{L}_0 := \frac{L_0}{d}$ . Now, solve this using the perturbative forms:

$$X(t) = 1 + \epsilon X_1(t) + \epsilon^2 X_2(t) + O(\epsilon^3), \quad (20)$$

$$Y(t) = 1 + \epsilon Y_1(t) + \epsilon^2 Y_2(t) + O(\epsilon^3). \quad (21)$$

Note

$$\frac{1}{Y} = 1 - \epsilon Y_1 + \epsilon^2 (-Y_2 + Y_1^2) + O(\epsilon^3). \quad (22)$$

Therefore, by collecting  $O(\epsilon)$  in Eq. (19),

$$\dot{X}_1 = \alpha [m(t) - X_1], \quad (23a)$$

$$\dot{Y}_1 = \beta [h(t) - Y_1], \quad (23b)$$

where  $\alpha := \frac{k}{\gamma}(\frac{3a}{2d} + 1)$ ,  $\beta := \frac{k}{\gamma}(-\frac{3a}{2d} + 1)$ ,  $m(t) := \sin \phi_1 + \sin \phi_2$ , and  $h(t) := \sin \phi_2 - \sin \phi_1$ . Similarly, for  $O(\epsilon^2)$ ,

$$\dot{X}_2 = -\frac{3akY_1}{2\gamma d} [m(t) - X_1] - \alpha X_2, \quad (24a)$$

$$\dot{Y}_2 = \frac{3akY_1}{2\gamma d} [h(t) - Y_1] - \beta Y_2. \quad (24b)$$

Solving these equations, the time-asymptotic expressions are obtained as

$$X_1 = \frac{2\alpha \cos\left(\frac{\psi}{2}\right) \left[ \alpha \sin\left(\omega t + \frac{\psi}{2}\right) - \omega \cos\left(\omega t + \frac{\psi}{2}\right) \right]}{\alpha^2 + \omega^2}, \quad (25a)$$

$$Y_1 = \frac{2\beta \sin\left(\frac{\psi}{2}\right) \left[ \beta \cos\left(\omega t + \frac{\psi}{2}\right) + \omega \sin\left(\omega t + \frac{\psi}{2}\right) \right]}{\beta^2 + \omega^2}, \quad (25b)$$

$$X_2 = -\frac{3a\beta k\omega \sin(\psi)}{2\alpha\gamma d (\alpha^2 + \omega^2) (\alpha^2 + 4\omega^2) (\beta^2 + \omega^2)} \left[ (\alpha^2 + 4\omega^2) (\alpha\beta + \omega^2) + \alpha\omega (\alpha^2 + 3\alpha\beta - 2\omega^2) \sin(2\omega t + \psi) + \alpha (\alpha^2\beta - 3\alpha\omega^2 - 2\beta\omega^2) \cos(2\omega t + \psi) \right], \quad (25c)$$

$$Y_2 = -\frac{3a\beta k\omega \sin^2\left(\frac{\psi}{2}\right) \left[ (2\omega^3 - 4\beta^2\omega) \cos(2\omega t + \psi) + \beta (\beta^2 - 5\omega^2) \sin(2\omega t + \psi) \right]}{\gamma d (\beta^2 + \omega^2)^2 (\beta^2 + 4\omega^2)}. \quad (25d)$$

With these expressions, one may now calculate  $R$  and  $W$ . Substituting Eq. (25) into Eq. (11),

$$R = \frac{9\pi a^2 k^2 \sin(\psi) \beta (\alpha\beta + \omega^2)}{2l\gamma^2 \alpha (\alpha^2 + \omega^2) (\beta^2 + \omega^2)} \epsilon^2 [1 + O(\epsilon)] \quad (26)$$

which vanishes in the first order of  $\epsilon$  while generally not in the second order of  $\epsilon$  (cf. Eq. (10) and Eq. (25)). Substituting Eq. (25) into Eq. (12) and using  $F_1^2 + F_2^2 = \frac{(F_1+F_2)^2 + (F_1-F_2)^2}{2}$ ,

$$W = \frac{\pi k^2 \omega d^2 \left[ (\beta^2 - \alpha^2) \cos(\psi) + \alpha^2 + \beta^2 + 2\omega^2 \right]}{\gamma (\alpha^2 + \omega^2) (\beta^2 + \omega^2)} \epsilon^2 [1 + O(\epsilon)] \quad (27)$$

which implies similar minimal energy dissipation versus phase difference as in Ref. [20]. Therefore,

$$\eta = \frac{81a^4 \beta^2 k^2 \sin^2(\psi) (\alpha\beta + \omega^2)^2}{16\gamma^2 \alpha^2 d^2 l^2 (\alpha^2 + \omega^2) (\beta^2 + \omega^2) \left[ (\beta^2 - \alpha^2) \cos(\psi) + \alpha^2 + \beta^2 + 2\omega^2 \right]} \epsilon^2 [1 + O(\epsilon)]. \quad (28)$$

It should be noted that all quantities start from  $O(\epsilon^2)$  because the contributions of first-order terms are averaged out over one cycle. As shown in Fig. 3, these expressions are in excellent agreement with the simulation results.

Furthermore, by recalling that  $\frac{a}{d}$  is assumed to be small and using  $\alpha = \beta = \frac{k}{\gamma} + O(\frac{a}{d})$ , the expressions can be much simplified as

$$R = \frac{9\pi a^2 L_0^2 k^2 \sin(\psi)}{2ld^2 (k^2 + \gamma^2 \omega^2)} \epsilon^2 \left[ 1 + O\left(\epsilon, \frac{a}{d}\right) \right], \quad (29a)$$

$$W = \frac{2\pi L_0^2 k^2 \omega \gamma}{(k^2 + \gamma^2 \omega^2)} \epsilon^2 \left[ 1 + O\left(\epsilon, \frac{a}{d}\right) \right], \quad (29b)$$

$$\eta = \frac{81a^4 L_0^2 k^2 \sin^2(\psi)}{32l^2 d^4 (k^2 + \gamma^2 \omega^2)} \epsilon^2 \left[ 1 + O\left(\epsilon, \frac{a}{d}\right) \right]. \quad (29c)$$

From these expressions, observe that  $R$  decreases with increasing  $d$ , proportionally to  $1/d^2$ . Thus,  $R$  vanishes at a large  $d$  limit, indicating the essential role of hydrodynamic interaction on the generation of the net flow. In contrast,  $W$  is almost independent of  $d$  and the leading term is just the sum of the works of two independent beads; the hydrodynamic interaction gives little contribution to the work for  $d \gg a$ . Therefore,  $\eta$  is approximately proportional to  $R^2$  and its maxima approximately coincide with the maxima of  $R$ .

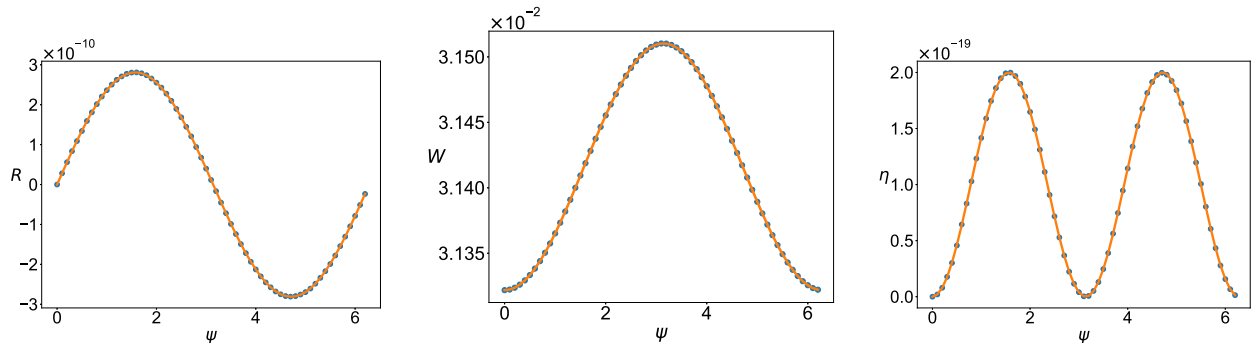


FIG. 3. The net transportation  $R$  and the work  $W$  over one cycle as well as the efficiency  $\eta$  with respect to the phase difference  $\psi$  in the two-bead case ( $N = 2$ ). Solid curves are the theoretical ones given in Eq. (26)–(28) while blue dots are the simulation results of Eq. (1) and Eq. (4). Parameter values:  $d = 50$ ,  $l = 1000$ , and  $\epsilon = 0.1$ .

#### IV. MULTIPLE BEAD CASE

In this section, a more general setup is considered, where the number of bead  $N$  is no longer restricted by two. In the simulation, we set  $\psi_i = i\Delta\psi$ , where  $\Delta\psi$  is a constant describing the phase difference. In this setup, one only needs to consider  $0 \leq \Delta\psi \leq \pi$  because of the symmetry of the system. Such a pattern mimics the metachronal wave ubiquitously found in the collective motion of flagella or cilia (cf. Ref. [30]). For  $N = 3$ , as shown in Fig. 4, this setup is numerically proven to approximately produce the maximum efficiency output for the cases of  $N = 3$ . The figure represents the efficiency as a function of  $\psi_2$  and  $\psi_3$ , in which the optimality is found at  $(\psi_2, \psi_3) \approx (1.3, 2.6)$ , thus  $\psi_3 \approx 2\psi_2$ .

We first observe the dependence of per-unit efficiency  $\eta$  on  $\Delta\psi$ , shown in Fig. 5(a). It is seen that the optimal phase difference, denoted as  $\Delta\psi^*$ , decreases as  $N$  increases. In Fig. 5(b), we further plot the dependence of  $\Delta\psi^*$  on the bead number  $N$ , suggesting that  $\Delta\psi^*$  approaches a certain value as  $N$  increases. There, we test two different  $d$  values and find that the dependence on  $d$  is rather weak.

We then observe the  $N$ -dependencies of  $R$ ,  $W$  and  $\eta$  values for  $\Delta\psi = \Delta\psi^*$ , denoted as  $R^*$ ,  $W^*$ , and  $\eta^*$ , respectively. We plot these values in Fig. 6, where the vertical axes are scaled as  $R^* \frac{d^2}{\epsilon^2}$ ,  $W^* \frac{1}{\epsilon^2}$ , and  $\eta^* \frac{d^4}{\epsilon^2}$ . This scaling is motivated from the theoretical predicted dependence on  $d$  and  $\epsilon$  for  $N = 2$ , given in Eq. (29); i.e.,  $R \propto \frac{\epsilon^2}{d^2}$ ,  $W \propto \epsilon^2$ , and  $\eta \propto \frac{\epsilon^2}{d^4}$ . Figure 6(a) indicates that  $R$  increases approximately linearly with  $N$ , particularly for large  $d$ . Moreover, as shown in Fig. 6(b),  $W^*$  increases virtually linearly with  $N$ , indicating that the work was approximately equal to the summation of independent beads. Assuming  $R, W \propto N$ ,  $\eta = \frac{R^2}{W^2 N}$  should be independent of  $N$ ; however, as shown in Fig. 6(c),  $\eta$  is actually strongly dependent on  $N$ , indicating that the growth of  $R$  significantly deviates from a linear growth. Importantly,  $\eta$  for  $N > 2$  is larger than  $\eta$  for  $N = 2$ , indicating the positive cooperative effect of hydrodynamic coupling. It should also be noted that  $\eta$  saturates or even turns to decrease for large  $N$ , which could come from our simple setting for the phase offsets and can possibly be improved by considering a more complex pattern of  $\psi_i$ . It is also observed that all the quantities at given  $N$  in Fig. 6 have similar magnitudes, suggesting that the dependence  $R \propto \frac{\epsilon^2}{d^2}$ ,  $W \propto \epsilon^2$ , and  $\eta \propto \frac{\epsilon^2}{d^4}$  roughly holds true for  $N \geq 3$ .

#### V. CONCLUSION

We introduced a simple one-dimensional coupled sphere motor model, with the generated flow and transportation efficiency investigated both theoretically and numerically. For the minimal case with two beads, the proper theoretical expression for both the net transportation and the efficiency are derived by the perturbation method, and it is proven that these results are in excellent agreement with the numerical results. Furthermore, we numerically investigated the case of  $N \geq 3$  and found that the efficiency increases with  $N$ .

For a more practical usage, the effect of a wall, to which the system is pinned, should also be examined; such a setup can be treated by using the Blake tensor [17, 31] instead of the Oseen tensor. It could be very helpful to derive theoretical expressions for the net transportation and efficiency for this case. In our model, oscillators were designed non-autonomous for simplicity; to understand the role of synchronization and self-organized metachronal wave pattern, it is essential to extend the model to the case of autonomous oscillators and compose a theoretical framework. Such an

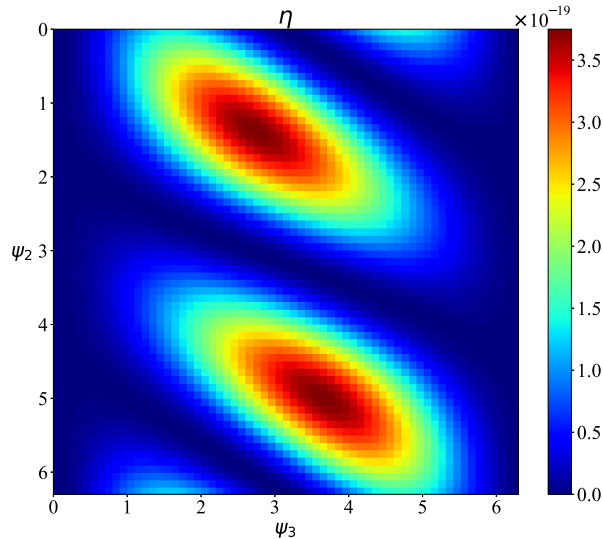


FIG. 4. Efficiency  $\eta$  of the three-bead system as a function of phase offsets  $\psi_2$  and  $\psi_3$  for  $N = 3$ . Parameter values are the same as those in Fig. 3.

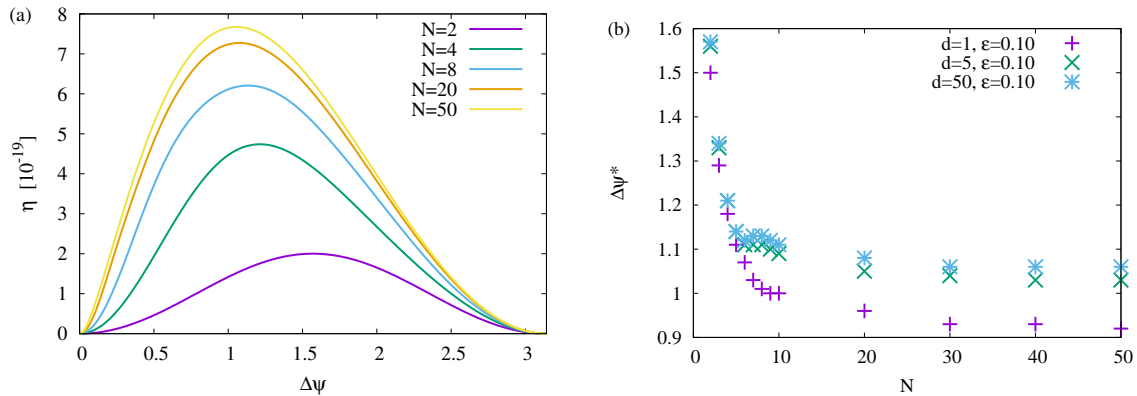


FIG. 5. (a) Per-unit efficiency  $\eta$  versus phase difference  $\Delta\psi$  in the  $N$ -beads cases. (b) Optimal phase difference  $\Delta\psi^*$  versus  $N$ .

effort would substantially contribute to deepening the understanding of the hydrodynamic effect of interactive objects in low Reynolds numbers. Moreover, it is worth discovering whether the higher order interactions will eventually destroy the positive coupling effect completely for very large number of oscillators, and if this is also true with effect of a wall. In addition, a two-dimensional movement model could be considered, as many other publications have focused, while the complexity in finding a theoretical expression could be fairly challenging.

- 
- [1] C. Brennen and H. Winet, Fluid mechanics of propulsion by cilia and flagella, *Annual Review of Fluid Mechanics* **9**, 339 (1977).
  - [2] K. M. Ottemann and J. F. Miller, Roles for motility in bacterial–host interactions, *Molecular microbiology* **24**, 1109 (1997).
  - [3] N. Falk, M. Lösl, N. Schröder, and A. Gießl, Specialized cilia in mammalian sensory systems, *Cells* **4**, 500 (2015).
  - [4] S. Ramaswamy, The mechanics and statistics of active matter, *Annu. Rev. Condens. Matter Phys.* **1**, 323 (2010).
  - [5] B. Friedrich, Hydrodynamic synchronization of flagellar oscillators, *The European Physical Journal Special Topics* **225**, 2353 (2016).
  - [6] H. Berg, *Random walks in biology* (expanded ed.) princeton university press, Princeton, NJ (1993).
  - [7] G. I. Taylor, Analysis of the swimming of microscopic organisms, *Proceedings of the Royal Society of London. Series A. Mathematical and Physical Sciences* **209**, 447 (1951).

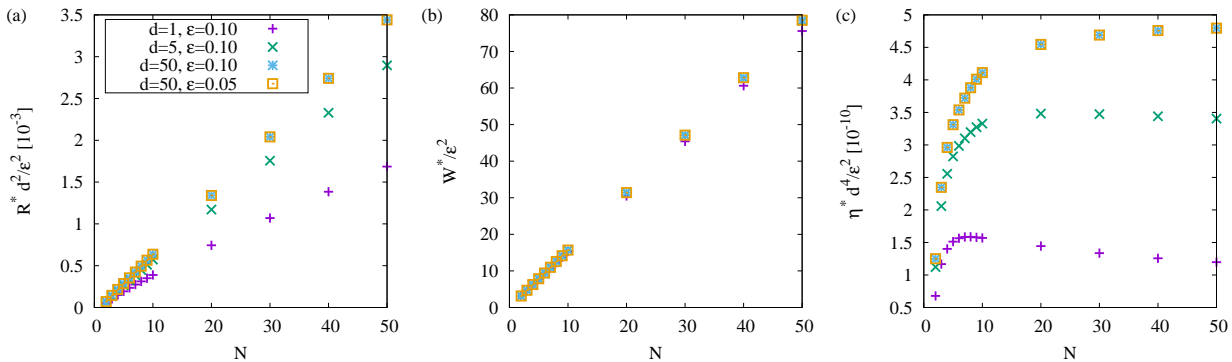


FIG. 6. Net transportation  $R^*$ , work  $W^*$ , and per-unit efficiency  $\eta^*$  for optimal phase difference  $\Delta\psi^*$  as functions of  $N$ .

- [8] N. Darnton, L. Turner, K. Breuer, and H. C. Berg, Moving fluid with bacterial carpets, *Biophysical journal* **86**, 1863 (2004).
- [9] N. Coq, A. Bricard, F.-D. Delapierre, L. Malaquin, O. Du Roure, M. Fermigier, and D. Bartolo, Collective beating of artificial microcilia, *Physical review letters* **107**, 014501 (2011).
- [10] A. Shields, B. Fiser, B. Evans, M. Falvo, S. Washburn, and R. Superfine, Biomimetic cilia arrays generate simultaneous pumping and mixing regimes, *Proceedings of the National Academy of Sciences* **107**, 15670 (2010).
- [11] M. Vilfan, A. Potočnik, B. Kavčič, N. Osterman, I. Poberaj, A. Vilfan, and D. Babič, Self-assembled artificial cilia, *Proceedings of the National Academy of Sciences* **107**, 1844 (2010).
- [12] S. Michelin and E. Lauga, Efficiency optimization and symmetry-breaking in a model of ciliary locomotion, *Physics of fluids* **22**, 111901 (2010).
- [13] E. Lauga, Bacterial hydrodynamics, arXiv preprint arXiv:1509.02184 (2015).
- [14] B. M. Friedrich and F. Jülicher, Flagellar synchronization independent of hydrodynamic interactions, *Physical Review Letters* **109**, 138102 (2012).
- [15] N. Uchida and R. Golestanian, Generic conditions for hydrodynamic synchronization, *Physical Review Letters* **106**, 058104 (2011).
- [16] A. Chamolly and E. Lauga, Direct versus indirect hydrodynamic interactions during bundle formation of bacterial flagella, *Physical Review Fluids* **5**, 123102 (2020).
- [17] N. Uchida and R. Golestanian, Hydrodynamic synchronization between objects with cyclic rigid trajectories, *The European Physical Journal E* **35**, 1 (2012).
- [18] J. Kotar, L. Debono, N. Bruot, S. Box, D. Phillips, S. Simpson, S. Hanna, and P. Cicuta, Optimal hydrodynamic synchronization of colloidal rotors, *Physical Review Letters* **111**, 228103 (2013).
- [19] T. Niedermayer, B. Eckhardt, and P. Lenz, Synchronization, phase locking, and metachronal wave formation in ciliary chains, *Chaos: An Interdisciplinary Journal of Nonlinear Science* **18**, 037128 (2008).
- [20] W. Liao and E. Lauga, Energetics of synchronization for model flagella and cilia, *Physical Review E* **103**, 042419 (2021).
- [21] M. A. Sleight, J. R. Blake, and N. Liron, The propulsion of mucus by cilia, *American Review of Respiratory Disease* **137**, 726 (1988).
- [22] L. E. Kuek and R. J. Lee, First contact: the role of respiratory cilia in host-pathogen interactions in the airways, *American Journal of Physiology-Lung Cellular and Molecular Physiology* **319**, L603 (2020).
- [23] E. Bianchi, Y. Sun, A. Almansa-Ordenez, M. Woods, D. Goulding, N. Martinez-Martin, and G. J. Wright, Control of oviductal fluid flow by the g-protein coupled receptor *adgrd1* is essential for murine embryo transit, *Nature communications* **12**, 1251 (2021).
- [24] N. Osterman and A. Vilfan, Finding the ciliary beating pattern with optimal efficiency, *Proceedings of the National Academy of Sciences* **108**, 15727 (2011).
- [25] N. Naremsatsu, R. Quek, K.-H. Chiam, and Y. Iwamoto, Ciliary metachronal wave propagation on the compliant surface of paramecium cells, *Cytoskeleton* **72**, 633 (2015).
- [26] J. Dhont, *An Introduction to Dynamics of Colloids*, ISSN (Elsevier Science, 1996).
- [27] M. Lighthill, On the squirming motion of nearly spherical deformable bodies through liquids at very small reynolds numbers, *Communications on pure and applied mathematics* **5**, 109 (1952).
- [28] A. M. Leshansky, O. Kenneth, O. Gat, and J. E. Avron, A frictionless microswimmer, *New Journal of Physics* **9**, 145 (2007).
- [29] R. Golestanian and A. Ajdari, Analytic results for the three-sphere swimmer at low reynolds number, *Physical Review E* **77**, 036308 (2008).
- [30] J. Elgeti, R. G. Winkler, and G. Gompper, Physics of microswimmers—single particle motion and collective behavior: a review, *Reports on progress in physics* **78**, 056601 (2015).
- [31] J. Blake, A model for the micro-structure in ciliated organisms, *Journal of Fluid Mechanics* **55**, 1 (1972).